Philosophical Magazine A
Publication details, including instructions for authors and subscription information:
http://www.tandfonline.com/loi/tpha20

Inelastic scattering probabilities in scanning transmission electron microscopy

R. H. Ritchie [a c] & A. Howie [b]

[a] Oak Ridge National Laboratory, P.O. Box 2008, Oak Ridge, Tennessee, 37831-6123, U.S.A.

[b] Cavendish Laboratory, Madingley Road, Cambridge, CB3 0HE, England

[c] Also Department of Physics, The University of Tennessee, Knoxville, Tennessee, 37996, U.S.A.

Available online: 20 Aug 2006

To cite this article: R. H. Ritchie & A. Howie (1988): Inelastic scattering probabilities in scanning transmission electron microscopy, Philosophical Magazine A, 58:5, 753-767

To link to this article: http://dx.doi.org/10.1080/01418618808209951

PHILOSOPHICAL MAGAZINE A, 1988, VOL. 58, NO. 5, 753–767

Inelastic scattering probabilities in scanning transmission electron microscopy†

By R. H. RITCHIE‡

P.O. Box 2008, Oak Ridge National Laboratory,
Oak Ridge, Tennessee 37831-6123, U.S.A.

and A. HOWIE

Cavendish Laboratory, Madingley Road, Cambridge CB3 0HE, England

[*Received 22 July 1987§ and accepted 22 January 1988*]

ABSTRACT

In this paper, we derive a general expression for the excitation probability corresponding to the collection of inelastically scattered electrons in a scanning transmission electronic microscopy configuration. We prove that, if all inelastically scattered electrons are collected, then the fraction of electrons that will be determined to have given rise to excitation in a localized target at impact parameter b may be calculated by simply convoluting over b (1) the probability $P^c(\mathbf{b})$ that a classical electron with the same velocity well create the excitation at given b, with (2) the probability of finding the electron in the microprobe at that impact parameter. We also show that, even in the opposite extreme, when a small solid angle of axial collection is employed, the energy-loss spectrum will still approximate to the classical expression provided that it is normalized to the same zero-loss intensity and if the Fourier-transformed profile function does not become too small for some ranges of its argument. A realistic microprobe distribution is used to compute the angular distribution of electrons that have created a surface plasmon or a surface optical phonon at a surface parallel to the electron trajectory. The results demonstrate the usefulness of the classical theory for axial detector positions as well as the possibility of enhanced spatial resolution for off-axis detector positions.

§ 1. INTRODUCTION

As a result of recent developments in scanning transmission electron microscopy (STEM), it is now possible routinely to study electronic excitation of inhomogeneous systems in highly localized regions (see for example Issacson and Johnson (1975), Joy (1979), Egerton (1980), Brown (1981)). This is achieved by recording changes in energy-loss distributions measured when a well focused, approximately 0·5 nm probe of swift (about 80 keV) electrons is scanned slowly across a specimen. The energy-loss spectra are generally produced in a spectrometer with a relatively small solid angle of acceptance at a scattering angle which can be varied. Although the technique of localized electron energy loss spectroscopy was applied many years ago in conventional electron microscopes (for a review, see Metherell (1971)), its implementation and extension to the higher characteristic losses associated with inner-shell excitations are much easier by STEM. However, in view of the reciprocity

† The submitted manuscript has been authored by a contractor of the U.S. Government under contract No. DE-AC05-84OR21400. Accordingly, the U.S. Government retains a non-exclusive, royalty-free license to publish or reproduce the published form of this contribution, or allow others to do so, for U.S. Government purposes.

‡ Also Department of Physics, The University of Tennessee, Knoxville, Tennessee 37996, U.S.A.

§ Received in present form 18 December 1987.

principle linking the two instruments, the arguments of this paper can be applied equally well in both situations.

The interpretation of these data raises a number of problems connected with the description and localization of excitations in inhomogeneous systems (Ritchie (1981), hereafter referred to as I, Batson (1982 a), Colliex (1985)). In addition, the interaction involves the wave–particle duality of the fast electron in an interesting context. The treatments of localized excitations in periodic crystalline media have used a fairly broad beam wave-mechanical description for the fast-electron states (Craven, Gibson, Howie and Spalding 1978, Taftø, Krivanek, Spence and Honig 1982), whereas studies of excitations in other systems containing particles (Batson 1980, 1982 b, Schmeits 1981, Das and Gersten 1983, Ferrell and Echenique 1985, Echenique and Howie 1985, Echenique, Bausells and Rivacoba 1987) or interfaces (Krivanek, Tanishiro, Takayanagi and Yagi 1983, Howie and Milne 1985, Echenique and Pendry 1975) have usually employed a classical description of the fast electron together with dielectric response theory for the solid. Howie, Linington and Tomlinson (1971) considered matrix elements between an initial electron probe wavefunction, localized in one dimension, and a final plane wavefunction in connection with channelling effects in STEM. The effects of spatial dispersion have been discussed, within the specular reflection model of Ritchie and Marusak (1966) by Echenique (1985). Wave-mechanical calculation of the excitation of dipole surface plasmons by a localized probe has been made by Kohl (1983, 1985). Recently, Echenique *et al.* (1987) have presented a quantum self-energy approach to the energy-loss problem in electron microscopy.

Here we explore the relation between the wave and the particle pictures, building on an earlier paper I which dealt with the case of broad-beam coherent irradiation of the target. In I, it was shown that energy analysis of swift imaged electrons which have generated localized electronic excitations in the target gives nearly the same result as if the electrons were classical projectiles moving on rectilinear trajectories and with a uniform distribution in impact parameter. This equivalence is more accurately satisfied the higher the electron's speed. An expression for the quantal correction to this prescription was derived and evaluated in some simple cases. The correction was found to be small for electrons with energies much greater than the energy lost to the target.

In this paper, we generalize the result given in I. We study the distribution of energy loss and angular deflection when the incident electron is prepared in microprobe form and is allowed to interact with a localized electronic system. First-order perturbation theory is employed throughout. We derive an expression for the excitation probability determined when inelastically scattered electrons are collected in an arbitrary direction. The microprobe is at a specified distance from the region in which excitation occurs. We prove that, when the collector is large enough that essentially all inelastically scattered electrons are detected, the probability of the excitation may be calculated by simply convoluting, over impact parameter, the probability that a classical electron with the same velocity will create the excitation at given impact parameter with the probability of finding the electron in the microprobe at that impact parameter. We note that the implication that all inelastically scattered electrons are collected is present in the analysis in I but is not stated explicitly. We also derive an expression for the size of the angle which must be subtended by the collector at the target in order than this equivalence shall be satisfied.

In § 4, we deal with the case of a very small solid angle of collection where once again a simple relation between the quantal and the classical results appears likely to hold.

Finally, in § 5, we illustrate some of these points with detailed calculations for the generation of surface or interface excitations, exploring the range of validity of the classical approximation and the possibility of improved spatial resolution for off-axis detector positions.

§ 2. Excitation of electronic transitions by a swift classical electron

Consider a classical electron with constant velocity $\mathbf{v}$ and interacting with excitations in an arbitrary target. The Coulomb interaction energy between the projectile and electrons in the target at time t may be written

$$H'(t)=\sum_{j=1}^{N}\frac{e^2}{|\mathbf{r}(t)-\mathbf{r}_j|}. \tag{1}$$

Here $\mathbf{r}_j$ is the coordinate of the jth electron in the N-electron target and $\mathbf{r}(t)=\mathbf{b}+\mathbf{v}t$, where $\mathbf{b}$ is the impact parameter relative to some origin in the target ($\mathbf{b}\cdot\mathbf{v}=0$).

First-order perturbation theory gives a simple expression for the probability $P_n(\mathbf{b})$ that the target will be excited from its ground state to its nth state in the course of the collision. This is

$$P_n^{\mathrm{c}}(\mathbf{b})=\left|\frac{1}{\mathrm{i}\hbar}\int_{-\infty}^{\infty}\mathrm{d}t\exp(\mathrm{i}\omega_{n0}t)\langle n|H'(t)|0\rangle\right|^2 \tag{2}$$

$$=\left(\frac{e^2}{\pi\hbar v}\right)^2\left|\int\frac{\mathrm{d}^2Q\exp(-\mathrm{i}\mathbf{Q}\cdot\mathbf{b})}{Q^2+\omega_{n0}^2/v^2}\rho_{n0}\left(\mathbf{Q},\frac{\omega_{n0}}{v}\right)\right|^2. \tag{3}$$

Equation (3) follows from eqn. (2) by using the Bethe integral

$$r^{-1}=(1/2\pi^2)\int\mathrm{d}^3q\exp(\mathrm{i}\mathbf{q}\cdot\mathbf{r})/q^2$$

and defining the matrix element of the density operator $\rho_{n0}(\mathbf{q})$ as

$$\rho_{n0}(\mathbf{q})=\left\langle n\left|\sum_{j=1}^{N}\exp(\mathrm{i}\mathbf{q}\cdot\mathbf{r}_j)\right|0\right\rangle. \tag{4}$$

This expectation value is taken between the nth excited state with state vector $|n\rangle$ and eigenenergy E_n and the ground state with eigenstate and eigenenergy $|0\rangle$ and E_0 respectively. The energy difference $E_n-E_0\equiv\hbar\omega_{n0}$. In eqn. (3) the vector $\hbar\mathbf{q}$ representing momentum transfer to the target is resolved into components $\mathbf{Q}$ and $q_z=\omega_{n0}/v$ such that $\mathbf{Q}\cdot\mathbf{v}=0$. Similarly, $\mathbf{r}=(\boldsymbol{\rho},z)$.

§ 3. Excitation of electronic transitions by a microprobe electron

Now we consider excitation of the target by an electron prepared in the form of a narrow beam. Figure 1 shows a schematic representation of a typical STEM configuration. The electron may be represented by the wave packet

$$\psi_0(\mathbf{r})=\frac{1}{(2\pi)^2}\int\mathrm{d}^2Q\,\phi_{\mathbf{Q}}\exp[\mathrm{i}\mathbf{Q}\cdot(\boldsymbol{\rho}-\mathbf{b})]\{\exp[\mathrm{i}z(k_0^2-Q^2)^{1/2}]\}/L^{1/2}, \tag{5}$$

where $\phi_{\mathbf{Q}}$ is chosen such that at $z=0$ the packet is distributed about the impact parameter $\mathbf{b}$ in a narrow probe with spatial extension Δ. For example, one might choose $\phi_{\mathbf{Q}}=(2\pi\Delta^2)^{1/2}\exp(-\Delta^2Q^2/4)$ corresponding to a Gaussian probability in $\boldsymbol{\rho}=(x,y)$, i.e. $\phi(\boldsymbol{\rho})=(2/\pi\Delta^2)^{1/2}\exp(-\rho^2/\Delta^2)$. We take $k_0=mv/\hbar$ and normalize

Fig. 1

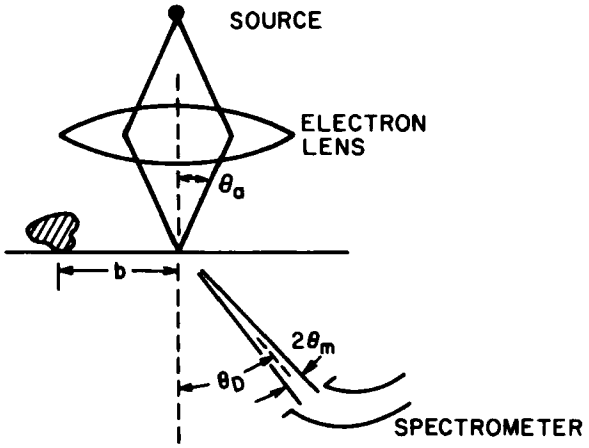

Schematic illustration of apparatus used in measuring inelastic scattering in STEM geometry. The object is located at average impact parameter b from the centre of the beam and scattered electrons are collected at angle θ_D with respect to the beam. The angle subtended by the collector at the object is θ_m, and θ_a is the maximum probe convergence angle.

the electron wavefunction in the length L in the z direction. With the relation $\phi(\rho)=(2\pi)^{-2}\int d^2Q\,\phi_{\mathbf{Q}}\exp(i\mathbf{Q}\cdot\rho)$, it follows that $\int d^2Q\,|\phi_{\mathbf{Q}}|^2=(2\pi)^2$.

Equation (5) represents a superposition of monoenergetic plane waves. Since we shall consider targets located near the plane $z=0$ and so thin that dispersion of the wave packet may be neglected in traversal of the targets, we shall neglect Q^2 compared with k_0^2 in eqn. (5). Thus, to a good approximation for our purposes,

$$\psi_0(\mathbf{r})=\phi(\rho-\mathbf{b})\exp(izk_0)/\sqrt{L}. \tag{6}$$

Let the microprobe pass close to a target located near the plane $z=0$. Golden rule theory predicts that the rate γ_n at which transitions to the nth excited state will occur is

$$\gamma_n=\frac{2\pi}{\hbar}\sum_{\mathbf{k}_f}\left|\int d^3r\frac{\exp(-i\mathbf{k}_f\cdot\mathbf{r})}{L^{3/2}}H'_{n0}\psi_0(\mathbf{r})\right|^2\delta\left(\frac{\hbar^2}{2m}(\mathbf{k}_0^2-\mathbf{k}_f^2)-\hbar\omega_{n0}\right). \tag{7}$$

The Hamiltonian H' in time-independent perturbation theory is

$$H'=\sum_{j=1}^{N}\frac{e^2}{|\mathbf{r}-\mathbf{r}_j|}. \tag{8}$$

and a typical final state of the electron after exciting the target is taken as $\psi_f(\mathbf{r})=\exp(i\mathbf{k}_f\cdot\mathbf{r})/L^{3/2}$ with energy $E_f=\hbar^2k_f^2/2m$. The energy of the initial state $\psi_0(\mathbf{r})$ is assumed to reside mainly in motion along the z axis ($k_0\gg 1/\Delta$) so that $E_0=\hbar^2k_0^2/2m$ in good approximation. Further, we assume that the energy difference

$$\varepsilon_0-\varepsilon_f=(\hbar^2/2m)(\mathbf{k}_0^2-\mathbf{k}_f^2)=\hbar v(k_0-k_{fz})+(\hbar^2/2m)\mathbf{k}_{f\rho}^2$$

and henceforth neglect the recoil term $(\hbar^2/2m)\mathbf{k}_{f\rho}^2$. This neglect should result in negligible error in STEM work as long as only valence electrons are excited. Recoil corrections were considered in I and were shown to be small at energies of interest.

Again using the Bethe integral form for the Coulomb interaction term, one finds from eqn. (7) that

$$\gamma_n=\frac{2\pi}{\hbar^2}\sum_{\mathbf{k_f}}\left|\int d^2\rho\,\phi(\boldsymbol{\rho}-\mathbf{b})\sum_{\mathbf{q}}\frac{4\pi e^2}{L^3q^2}\exp(i\mathbf{q}\cdot\mathbf{r})\rho_{n0}(\mathbf{q})\int_{-L/2}^{L/2}dz\exp[i(k_0z-\mathbf{k_f}\cdot\mathbf{r})]\right|^2 \times\delta[\omega_{n0}-v(k_0-k_{fz})]. \quad (9)$$

The transition probability P_n^q is given by the product of the transition rate γ_n and the interaction time L/v in the normalization used here. Thus after taking the limit $L\to\infty$ and expressing all sums as integrals in that limit, we find that

$$P_n^q=\left(\frac{e^2}{2\pi^2\hbar v}\right)^2 \times\int d^2k_{f\rho}\left|\int d^2\rho\,\phi(\boldsymbol{\rho}-\mathbf{b})\exp(-i\mathbf{k}_{f\rho}\cdot\boldsymbol{\rho})\int\frac{d^2Q\exp(-i\mathbf{Q}\cdot\boldsymbol{\rho})}{Q^2+\omega_{n0}^2/v^2}\rho_{n0}\left(\mathbf{Q},\frac{\omega_{n0}}{v}\right)\right|^2. \quad (10)$$

Extending the integral over $\mathbf{k}_{f\rho}$ to cover an infinite range of the two-dimensional variable $\mathbf{k}_{f\rho}$ (see Howie *et al.* (1971)) and using the identity

$$\int d^2k_{f\rho}\exp[-i\mathbf{k}_{f\rho}\cdot(\boldsymbol{\rho}-\boldsymbol{\rho}')]=4\pi^2\delta^2(\boldsymbol{\rho}-\boldsymbol{\rho}'),$$

we find that

$$P_n^q(\mathbf{b})=\int d^2\rho|\phi(\boldsymbol{\rho}-\mathbf{b})|^2P_n^c(\boldsymbol{\rho}). \quad (11)$$

This shows that, when all inelastically scattered electrons are collected, the measured probability of exciting a given transition may be computed theoretically as if the microprobe consisted of an incoherent superposition of classical trajectories distributed laterally to the beam direction according to the probability density $|\phi(\boldsymbol{\rho}-\mathbf{b})|^2$. This is a generalization of the result proved in I for an incident plane-wave electron.

We now consider how large the angle subtended by an axial detector at the scattering region must be in order that the closure approximation, eqns. (10) and (11), shall be valid. If the integral over $\mathbf{k}_{f\rho}$ in eqn. (10) is carried out over a large but finite range, the resulting function will be strongly peaked about the point $\boldsymbol{\rho}=\mathbf{b}$ and will have a width of about $1/k_m$, where k_m is the maximum wave-vector accepted by the detector. By comparison, the function ϕ varies appreciably over the characteristic distance Δ, while the ρ-dependent function

$$A_n(\boldsymbol{\rho})=\int\frac{d^2Q\exp(-i\mathbf{Q}\cdot\boldsymbol{\rho})}{Q^2+\omega_{n0}^2/v^2}\rho_{n0}\left(\mathbf{Q},\frac{\omega_{n0}}{v}\right) \quad (12)$$

appearing in the integrand of eqn. (10) is expected to have spatial extension of about v/ω_{n0}. Thus, if the inequality

$$1/k_m\ll\min(\Delta,v/\omega_{n0}) \quad (13)$$

is satisfied, the closure approximation should be excellent. If we take $k_m\approx k_0\theta_m$, where θ_m is the half-angle subtended by the detector at the scattering region, assuming it to be centred about the forward direction, and if we consider a microprobe of 100 keV electrons with a beam radius of about 1 nm which excites electronic transitions with a

characteristic energy of about 13 eV, then $v/\omega_{n0} \approx 9$ nm, and $k_0\theta_m \approx 1620\theta_m\,\mathrm{nm}^{-1}$. Then we require that $\theta_m \gg 1$ mrad in order that eqn. (11) shall be valid. The classical approximation could therefore fail when the spectrometer semi-angle θ_m of acceptance is very small. In practice, however, the tendency is to maximize detection efficiency by taking $\theta_m \geqslant \theta_a \approx 8$ mrad where θ_a is the maximum probe convergence semi-angle. The incident probe is moreover unlikely to be fully coherent in that $\Delta > 1/k_0\theta_a$. Taken together, these conditions ensure the validity of eqn. (12) for excitation energies up to 100 keV and perhaps beyond. For the classical model to hold, the scattered electrons must effectively all lie within the angular spread of the incident beam, and virtually all of them should be collected by the detector.

§4. Cases of partial signal collection

When the detector semi-angle $\theta_m \ll \theta_a$ and only partial collection of the inelastically scattered electron signal occurs, it is convenient to omit the integral over k_f in eqn. (10) and to define the differential probability $\mathrm{d}P_n/\mathrm{d}\Omega$ as k_0^2 times the integrand of that equation. Thus,

$$\frac{\mathrm{d}P_n}{\mathrm{d}\Omega} = \frac{1}{(2\pi^2 a_0)^2}\left|\int \mathrm{d}^2\rho\, \phi(\boldsymbol{\rho}-\mathbf{b}) \exp(-\mathrm{i}\mathbf{k}_f\cdot\boldsymbol{\rho})\, A_n(\boldsymbol{\rho})\right|^2 \tag{14}$$

using eqn. (12). Here $\mathrm{d}\Omega$ is the differential solid angle subtended by the detector, $\mathbf{k}_{f\rho} = k_0(\theta_D \cos\phi, \theta_D \sin\phi)$ and $a_0 = \hbar^2/me^2$ is the first Bohr radius (see fig. 1). The detector is assumed to be placed on or near the axis. An alternative form of eqn. (14) is

$$\frac{\mathrm{d}P_n}{\mathrm{d}\Omega} = \frac{1}{(2\pi^2 a_0)^2}\left|\int \frac{\mathrm{d}^2Q}{Q^2+\omega_{n0}^2/v^2}\,\rho_{n0}\left(\mathbf{Q}, \frac{\omega_{n0}}{v}\right)\phi_{\mathbf{k}_{f\rho}+\mathbf{Q}} \exp\left[-\mathrm{i}(\mathbf{k}_{f\rho}+\mathbf{Q})\cdot\mathbf{b}\right]\right|^2, \tag{15}$$

where the expansion

$$\phi(\boldsymbol{\rho}) = \frac{1}{(2\pi)^2}\int \mathrm{d}^2Q\, \phi_{\mathbf{Q}} \exp(\mathrm{i}\mathbf{Q}\cdot\boldsymbol{\rho}) \tag{16}$$

has been used as in eqn. (5). Here $\phi_{\mathbf{Q}}$ is the Fourier transform of the beam profile function $\phi(\boldsymbol{\rho})$.

Another approximation may be useful in connection with eqn. (15). The range of Q over which the factor $\rho_{n0}/(Q^2+\omega_{n0}^2/v^2)$ is expected to be most significant is $Q \lesssim \omega_{n0}/v$. By comparison the beam profile transform ϕ_Q has extension of about $1/\Delta$ in the variable $\mathbf{Q}$. Using the values $\omega/v \approx 0{\cdot}1\,\mathrm{nm}^{-1}$ from the example quoted above, one sees that for some cases it will be sufficient to evaluate $\phi_{\mathbf{k}_{f\rho}+\mathbf{Q}}$ at $\mathbf{Q}=0$ and remove it from the integrand. Denoting this approximation as $(\mathrm{d}P_n/\mathrm{d}\Omega)_f$, we have

$$(\mathrm{d}P_n/\mathrm{d}\Omega)_f = (k_0/2\pi)^2 |\phi_{\mathbf{k}_{f\rho}}|^2 P_n^c(\mathbf{b}). \tag{17}$$

where $P_n^c(\mathbf{b})$ is given in eqn (3). The inelastic signal intensity collected by a small-aperture detector is thus equal to the probability of energy loss $\hbar\omega_{n0}$ by a classical electron passing the target at the mean position of the microprobe multiplied by a factor which may be recognized as the fraction of the incident probe intensity which the detector aperture would accept in the absence of any scattering. In other words, the energy-loss spectrum recorded by STEM in such a case will, if normalized to the same zero-loss intensity, closely approximate that of a classical electron.

Clearly the validity of the approximation just described depends on the fact that the typical angle of inelastic scattering is much less than the angular distribution of the

incident probe. Cases where the detector is placed at an angle θ_D to the axis greater than the maximum probe convergence angle θ_a defined by the illumination aperture (see § 5.1) are not covered directly by this kind of approximation unless perhaps one assumes that the specimen is thick enough for the energy-loss signal to arise from a combination of large-angle thermal diffuse scattering and small-angle inelastic scattering. $|\phi_{\mathbf{k}_0\rho}|^2$ would then refer to the angular distribution of the incident probe allowing for thermal diffuse scattering. Note also that the approximate result, eqn. (17), is independent of the size of the probe Δ as long as $\Delta < \min[v/\omega_{n0}, (k_0\theta_m)^{-1}]$.

§ 5. The creation of surface excitations by a microprobe electron

The operation of the approximations described above can be investigated in the simple but topical case of surface plasmon or surface optical phonon excitation. In this example, we can also study situations where thin specimens are employed and the detector is displaced from axis by an angle $\theta_D \gg \theta_m$ so that large-angle single inelastic scattering predominates. In the case of periodic media Taftø *et al.* (1982) showed that this technique allows the detection of excitations with a relatively high momentum whose excitation is characterized by correspondingly small impact parameters at specific points in the unit cell.

The interaction Hamiltonian H' in eqn. (1) may be written

$$H'(t) = e^2 \int \mathrm{d}^3 r' \frac{\hat{n}(\mathbf{r}')}{|\mathbf{r}(t) - \mathbf{r}'|}, \tag{18}$$

where $\hat{n}(\mathbf{r})$ is the number operator for the surface plasmon field. Equation (18) is appropriate when a fast classical electron with linear trajectory specified by $\mathbf{r}(t)$ interacts with collective electron states in solids. Then the probability P_n^c that the field oscillators will be excited from the ground state to the nth state in the course of the collision becomes

$$P_n^c = \left| \frac{1}{\mathrm{i}\hbar} \sum_{\mathbf{q}} \frac{4\pi e^2}{L^3 q^2} \exp(-\mathrm{i}\mathbf{q}\cdot\mathbf{b})\, 2\pi\delta(\omega_{n0} - \mathbf{q}\cdot\mathbf{v}) \rho_n^{SP}(\mathbf{q}) \right|^2, \tag{19}$$

where

$$\rho_n^{SP} = \langle n | \int \mathrm{d}^3 r \exp(\mathrm{i}\mathbf{q}\cdot\mathbf{r})\, \hat{n}(\mathbf{r}) | 0 \rangle, \tag{20}$$

and $|n\rangle$ is now the state vector of the nth excited state of the surface oscillator. Anticipating the use of cyclic boundary conditions in a large volume L^3, we have used the Bethe integral in the form

$$r^{-1} = (4\pi/L^3) \sum_{\mathbf{q}} \exp(-\mathrm{i}\mathbf{q}\cdot\mathbf{r})/q^2.$$

The electronic density operator for the surface plasmon field associated with a surface located at the plane $x = 0$ may be approximated as (Ritchie and Wilems 1969, Mahan 1974)

$$\hat{n}(\mathbf{r}) = \sum_{\boldsymbol{\kappa}} \alpha_\kappa \delta(x) \exp(\mathrm{i}\boldsymbol{\kappa}\cdot\mathbf{R}) (\hat{b}_\kappa + \hat{b}_{-\kappa}), \tag{21}$$

where $\boldsymbol{\kappa}$ and $\mathbf{R}$ are vectors parallel to the y–z plane and $\alpha_\kappa^2 = \hbar\omega_s \kappa / 4\pi A e^2$ for the surface plasmon. For surface optical phonons, α_κ^2 is multiplied by the factor

$$F = (\varepsilon_0 - 1)/(\varepsilon_0 + 1) - (\varepsilon_\infty - 1)/(\varepsilon_\infty + 1),$$

Fig. 2

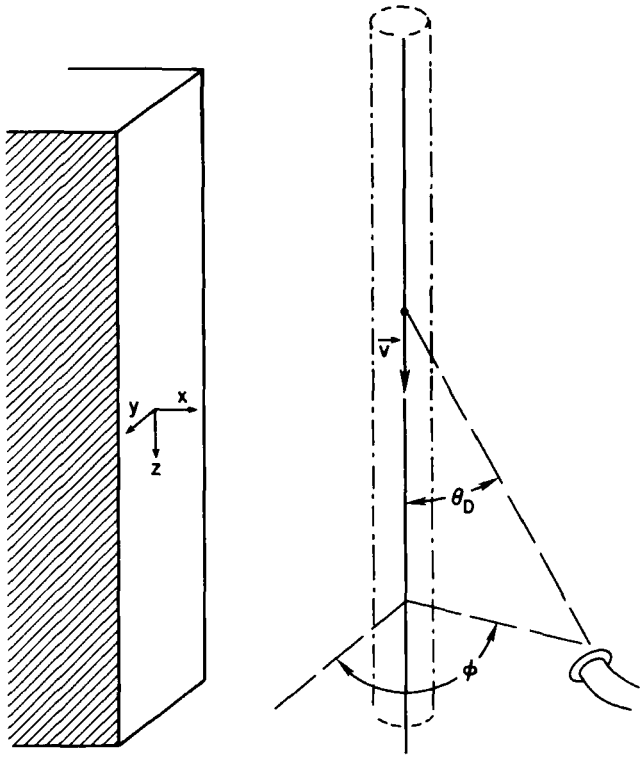

Schematic illustration of the geometry envisaged in the inelastic scattering of a microprobe electron through the angle (θ_D, ϕ) into a detector.

where ε_0 is the static dielectric constant of the lattice and ε_∞ is the dielectric constant at very high frequencies. The surface excitation energy is $\hbar\omega_s$ (assumed dispersionless), A is the area of the surface and $\hat{b}_\kappa$ is the annihilation operator for a surface excitation with wave-vector $\boldsymbol{\kappa}$. For definiteness, we take the trajectory parallel with the surface and at a distance b from it (fig. 2). Substituting eqn. (21) into eqn. (20) and carrying out the indicated integrations in eqn. (19), one finds that the probability $P^c_\kappa(\mathbf{b})$ of creating a surface quantum with energy $\hbar\omega_{n0}$ and momentum $\hbar\boldsymbol{\kappa}$ increases linearly with increasing time in the limit of a very large surface. Then, dividing the rate of surface mode creation by the velocity of the particle and summing over all $\boldsymbol{\kappa}$ yields $\mathrm{d}P^c/\mathrm{d}z$, the total probability of excitation per unit path length. Thus

$$\frac{\mathrm{d}P^c(b)}{\mathrm{d}z}=\frac{e^2\omega_s}{2\hbar v^2}\int_{-\infty}^{\infty}\mathrm{d}\kappa_y\frac{\exp(-2b\kappa)}{\kappa}=\frac{e^2\omega_s}{\hbar v^2}K_0\left(\frac{2b\omega_s}{v}\right), \tag{22}$$

where $K_0(z)$ is the modified Bessel function of the second kind and $\kappa=(\kappa_y^2+\omega_s^2/v^2)^{1/2}$. This agrees with the result obtained by Echenique and Pendry (1975) if one takes their expression for the imaginary part of the self-energy, eqn. (20), doubles the answer to go from probability amplitude to probability, and divides by v to obtain a probability per unit length. Note that it is not realistic to allow the momentum transfer $\hbar|\kappa_y|$ to become infinitely large in eqn. (22). An approximate correction to this equation may be obtained by replacing the limits $\pm\infty$ by the cut-off wavenumbers $\pm\kappa_c$, where

$\kappa_c \approx \omega_s/v_F$ for surface plasmons and v_F is the Fermi speed for the solid (see eqn. (28) below).

To treat the more general situation in which scattered electrons from the microprobe wave packet are collected in an arbitrary direction, we compute the differential probability $d^2P_n^q/dk_{f\rho}^2$, from eqn. (10) as

$$\frac{d^2P_n^q}{dk_{f\rho}^2}=\left(\frac{e^2}{2\pi^2\hbar v}\right)^2$$

$$\times\left|\int d^2\rho\,\phi(\boldsymbol{\rho}-\mathbf{b})\exp(-i\mathbf{k}_{f\rho}\cdot\boldsymbol{\rho})\int\frac{d^2Q\exp(-i\mathbf{Q}\cdot\boldsymbol{\rho})}{Q^2+\omega_{n0}^2/v^2}\rho_{n0}\left(\mathbf{Q},\frac{\omega_{n0}}{v}\right)\right|^2, \tag{23}$$

This is the differential probability that an electron in the microprobe shall acquire momentum $\mathbf{k}_{f\rho}=(k_{fx},k_{fy})$ in a direction perpendicular to $\mathbf{v}$ when the surface oscillators are excited to the nth state.

Using the expression for the electronic density operator correponding to the surface excitation field, eqn. (21), into eqn. (20), one finds

$$\rho_\kappa^{SP}=\alpha_\kappa(2\pi)^2\delta(\kappa_y-Q_y)\delta(\kappa_z-Q_z), \tag{24}$$

where the initial state vector $|0\rangle$ represents the vacuum state of the surface field and $|n\rangle=b_\kappa^+|0\rangle$, a state with a single excitation present. Note that hydrodynamic corrections to eqn. (21) (Ritchie and Wilems 1969) become important at distances of about 1 Å from the surface, where elastic scattering effects may become significant, as well. Again assuming that $\mathbf{v}$ is parallel to the y–z plane and that the centre of the microprobe is at a distance b from the surface, one may write

$$\frac{d^3P^q(b)}{dz\,dk_x\,dk_y}=\frac{e^2\omega_s}{8\pi^2\hbar v^2}\int_{-\infty}^{\infty}\frac{d\kappa_y}{\kappa}\left|\int d^2\rho\,\phi(\boldsymbol{\rho}-\mathbf{b})\exp(-ik_x x-\kappa|x|)\exp[i(\kappa_y-k_y)y]\right|^2. \tag{25}$$

Here the subscript on $\mathbf{k}_f$ has been dropped, and $\kappa=(\kappa_y^2+\omega_s^2/v^2)^{1/2}$. We ignore here elastic scattering of the probe wavefunction due to penetration of the medium (i.e. where $x<0$). For surface optical-phonon excitation, eqn. (25) should be multiplied by the dielectric factor F appearing just below eqn. (21). Equation (25) was obtained by summing over all momenta $\hbar\kappa$ of the surface excitation. We now investigate it for two specific beam profiles $\phi(\rho)$.

5.1. *Gaussian beam profile*

Using the Gaussian form $\phi(\rho)=(2/\pi\Delta^2)^{1/2}\exp(-\rho^2/\Delta^2)$, one finds that

$$\frac{d^3P_n^q(b)}{dz\,dk_x\,dk_y}=\frac{e^2\omega_s}{4\pi^2\hbar v^2}$$

$$\times\int_{-\infty}^{\infty}\frac{d\kappa_y}{\kappa}\exp\left(\frac{-\Delta^2(\kappa_y-k_y)^2}{2}\right)\left|\int_{-\infty}^{\infty}dx\exp\left(\frac{-(x-b)^2}{\Delta^2}\right)\exp(-ixk_x-\kappa|x|)\right|^2. \tag{26}$$

Equation (26) has been evaluated numerically for several different values of the scattering angles. For this purpose, it was convenient to make the following changes

in variables: $\kappa_y=(\omega_s \sinh\mu)/v$, $k_x=\omega_s\xi/v$, $k_y=\omega_s\eta/v$, $\delta=\omega_s\Delta/v$, $\bar{x}=\omega_s x/v$, $p=\mathrm{d}^3P_n^q(b)/\mathrm{d}z\,\mathrm{d}k_x\,\mathrm{d}k_y$. Then

$$p=\frac{e^2}{4\pi^2\hbar\omega_s}\int_{-\infty}^{\infty}\mathrm{d}\mu\exp\left(\frac{-\delta^2(\eta-\sinh\mu)^2}{2}\right)\left|\int_{-\infty}^{\infty}\mathrm{d}\bar{x}\exp\left(-\frac{\bar{x}^2}{\delta^2}\right)\right.$$
$$\left.\times\exp(-\mathrm{i}\xi\bar{x})\exp(-|\bar{x}+\bar{b}|\cosh\mu)\right|^2, \quad (27)$$

where $\bar{b}=b\omega_s/v$. One may show that by using the same approximations leading from eqn. (15) to eqn. (17), $\bar{p}$, an approximation to p, becomes

$$\bar{p}=(e^2\omega_s\Delta^2/2\pi\hbar v^2)\tilde{K}_0(2b\omega_s/v,\ v\kappa_c/\omega_s)\exp[-\Delta^2(k_x^2+k_y^2)/2]. \quad (28)$$

The function

$$\tilde{K}_0(x,y)=\int_0^{\sinh^{-1}y}\mathrm{d}\phi\exp(-x\cosh\phi),$$

and κ_c is the cut-off wave-vector for collective response of the system. For the surface plasmon $v\kappa_c/\omega_s\approx v/v_F$, where v_F is the Fermi speed of electrons in the metal. When $v/v_F\gg1$, $\tilde{K}_0(2\omega_s b/v,\ v\kappa_c/\omega_s)\to K_0(2\omega_s b/v)$, the modified Bessel function of the second kind and zero order. The ratio $R=p/\bar{p}$ is shown in fig. 3 as a function of $b\omega_s/v$ for several different values of η. To a good approximation the ratio R depends on the variable $(\xi^2+\eta^2)^{1/2}$; so only the angle η is specified for each curve. The azimuthal direction in fig. 2 is taken to have the components $\hbar\omega_s(\xi,\eta)/2E$. We have taken $\Delta\omega_s/v=0{\cdot}125$ for these calculations. It is seen that R is essentially unity when the microprobe has a small overlap with the region in which excitation occurs.

Fig. 3

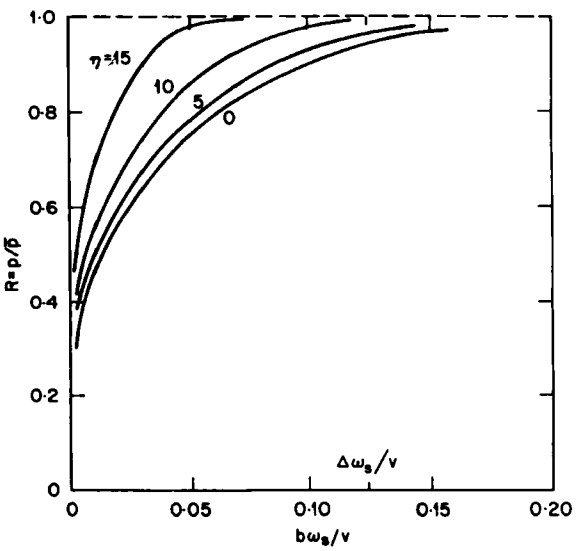

A plot of the ratio $R=p/\bar{p}$, where p and $\bar{p}$ are defined in eqns. (27) and (28), respectively, shown as a function of $\omega_s b/v$ for various directions of the collector with respect to the beam direction. The beam has been taken to have a Gaussian profile. The angle ϕ_D in fig. 2 is taken to have components $(\hbar\omega_s/2E)$ (ξ,η).

Equation (28) is an excellent approximation to eqn. (24) as long as $\Delta \ll v/\omega_s$, in which event the angular deflection of an electron in giving rise to a surface excitation is small compared with the intrinsic angular spread of the microprobe wave packet. In this limit, we may regard the microprobe as quasi-classical in that the dependence of loss probability on impact parameter is nearly that of eqn. (22), while the angular distribution reflects mainly the way that the beam is prepared.

In the other limit where $\Delta \gg v/\omega_s$, angular deflection accompanying energy loss will dominate the intrinsic spread, and the angular distribution will reduce to

$$\mathrm{d}P_n^q/\mathrm{d}\Omega = (e^2\theta_E/\pi\hbar v)[(\theta^2\cos^2\phi + \theta_E^2)^{1/2}/(\theta^2+\theta_E^2)^2], \tag{29}$$

where $\theta_E = \hbar\omega_s/mv^2$, θ is the polar angle between $\mathbf{v}$ and the direction of the scattered electron, and ϕ is the azimuthal scattering angle relative to the surface, that is $\kappa_y = k_0 \sin\theta\cos\phi$ and $\phi = 0$ corresponds to scattering in a direction parallel with the surface. We use the small-angle approximation, namely $\sin\theta \approx 0$.

Equation (26) can be used to investigate the case where the detector is displaced from axis by an angle θ_D, such that $k_y \gg 1/\Delta$. With some rather simple approximations, we then find that

$$p = (2^{1/2}e^2\omega_s/\pi^{3/2}\hbar v^2\Delta)[(k_y^2+\omega_s^2/v^2)^{1/2}/(k_x^2+k_y^2+\omega_s^2/v^2)^2]\exp\left(-2\frac{b^2}{\Delta^2}\right). \tag{30}$$

The spatial resolution achieved in the energy loss signal is now seen to be comparable with the probe size Δ which may be significantly better than the resolution v/ω_s attainable in the axial detector position. However, it is in many cases considerably greater than the resolution predicted by the classical expression (22) in the limit $\Delta \to 0$ where the finite probe size is ignored. Nevertheless the potential value of such off-axis experiments is demonstrated by this simple example.

We emphasize that, although the Gaussian profile contains unrealistically large momentum components, it should be qualitatively useful as long as $\theta_D \lesssim \theta_a$.

5.2. *Aperture function profile*

Better than a Gaussian function to represent a real wave-mechanical probe is the (normalized) wavefunction (Cowley 1982):

$$\phi_{\mathbf{Q}} = \frac{(4\pi)^{1/2}}{Q_a} H(Q_a - Q)\exp\left[\frac{\mathrm{i}}{\lambda}\left(\frac{\pi\Delta z}{k_0^2}Q^2 + \frac{\pi C_s Q^4}{2k_0^4}\right)\right], \tag{31}$$

where $Q_a = k_0\theta_a$, θ_a is the aperture semi-angle, $k_0 = 2\pi/\lambda = mv/\hbar$ and, as before, $\mathbf{v}$ is the electron velocity. C_s is the spherical aberration constant for the electron lens preceding the defining aperture, while Δz is the defocus distance and is usually taken as $\Delta z = (C_s\lambda)^{1/2}$ (Scherzer 1949). $H(x) = \frac{1}{2}(x/|x|+1)$ is the Heaviside step function. The function of eqn. (31) is more accurate than the Gaussian function used in eqn. (26) in that there are no Fourier components outside those accepted by the aperture.

After transforming variables, one finds that, if

$$\frac{\mathrm{d}^3P^q}{\mathrm{d}z\,\mathrm{d}k_x\,\mathrm{d}k_y} = \frac{m^2e^2\omega_s}{2\pi^3\hbar^3k_0^4\theta_a^2}p, \tag{32}$$

then

$$p = \int_{\alpha_-}^{\alpha_+}(1+\alpha^2)^{1/2}\,\mathrm{d}\alpha\left|\int_{\beta_-}^{\beta_+}\frac{\mathrm{d}\beta}{1+\alpha^2+\beta^2}\exp(-\mathrm{i}\bar{b}\beta)f(\beta)\right|^2, \tag{33}$$

where $\alpha_\pm = \pm\gamma_a + \eta$, $\beta_\pm = \pm[\gamma_a^2 - (\alpha-\eta)^2]^{1/2} - \xi$, $\bar{b} = b\omega_s/v$, $\gamma_a = vQ_a/\omega_s$ and $f(\beta)$ is the exponental factor in eqn. (31).

In many situations the phase shift due to the passage of the microprobe electron through the electron lens is negligible. The distribution function may be written in the alternative form, with $f(\beta)=1$, as

$$p(\bar{b},\xi,\eta)=\frac{1}{4}\int_{\alpha_-}^{\alpha_+}\frac{d\alpha}{s}\left|\int_{-\infty}^{\infty}\frac{dx}{x}\exp(-s|x-\bar{b}|)\,[\exp(ix\beta_+)-\exp(ix\beta_-)]\right|^2, \qquad (34)$$

where $s=(1+\alpha^2)^{1/2}$. A useful form for numerical calculation is obtained by deforming the contour in the inner integral of eqn. (33) with $f(\beta)=1$: one finds that

$$p=\int_{\alpha_-}^{\alpha_+} s\,d\alpha\left|\frac{\pi\exp(-bs)\,H(\beta_+)}{s}+i[I(\beta_-)-I(\beta_+)]\right|^2,$$

where

$$I(\beta)=\exp(i\bar{b}\beta)\int_0^\infty\frac{\exp(-\bar{b}y)\,dy}{s^2+(\beta+iy)^2}.$$

Note that for large $\bar{b}$ and β the integrand may oscillate rapidly as its argument varies in which case numerical convergence will be slow.

Fig. 4

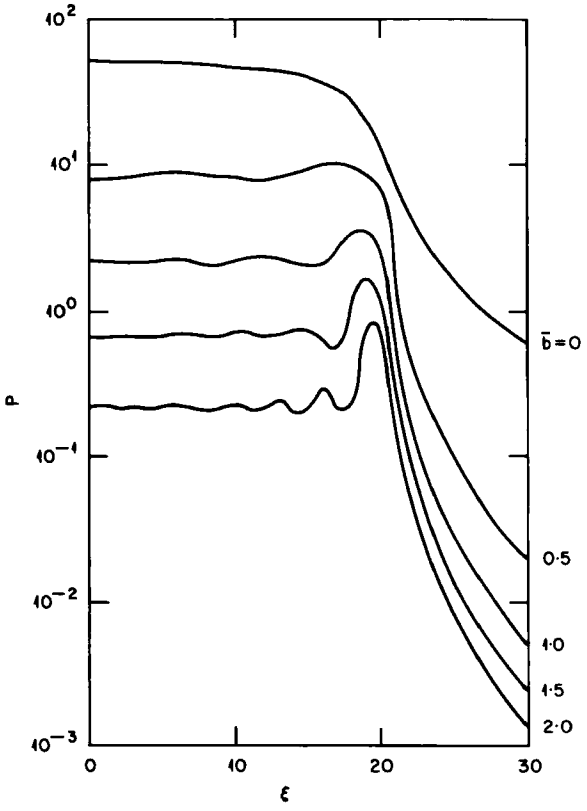

A plot of p, the differential probability of exciting a surface collective mode, as a function of the scaled collection angle $\xi = 2E\theta_x/\hbar\omega_s$ for the step function profile in eqn. (31), $\gamma_0 = 20$ and $\eta = 1$.

One may obtain single-integral approximations to this expression for the limiting cases $\bar{b}\to 0$ and for $\bar{b}\gg 1$. One obtains, for $\bar{b}\ll 1$,

$$p(0,\xi,\eta)=\int_{\theta_-}^{\theta_+} d\theta\,[\tan^{-1}(B_+)-\tan^{-1}(B_-)]^2, \tag{35}$$

where $\theta_\pm=\sinh^{-1}(\alpha_\pm)$ and $B_\pm=[\pm\{\gamma_a^2-(\sinh\theta-\eta)^2\}^{1/2}-\xi]/\cosh\theta$.

Figure 4 shows a plot of p as a function of ξ for several different values of $\bar{b}$ and for $\eta=1$, $\gamma_a=20$. This value of γ_a is appropriate to the excitation of surface plasmons and for $\theta_a\approx 1$ mrad. To reduce the complexity of the numerical computations, we have chosen θ_a to be unrealistically small. However, the qualitative nature of our conclusions should be unaffected. One sees a rapid decrease in p as the angle of collection exceeds that corresponding to forward scattering and pronounced fluctuations in p as ξ approaches γ_a from below and for the larger $\bar{b}$ values. Figure 5 shows p as a function of η for various $\bar{b}$ values and for $\xi=1$, $\gamma_a=20$. Figure 6 depicts the variation in p with $\bar{b}$ for various combinations of ξ and η and $\theta_a=20$. It appears that p tends to decrease more rapidly with increasing $\bar{b}$ when the collection angle increases in a direction perpendicular to the surface (increasing ξ) than when the collection angle increases parallel to the surface. This is qualitatively similar to the behaviour predicted by eqns. (29) and (30). It would be very interesting to check these predictions experimentally.

Fig. 5

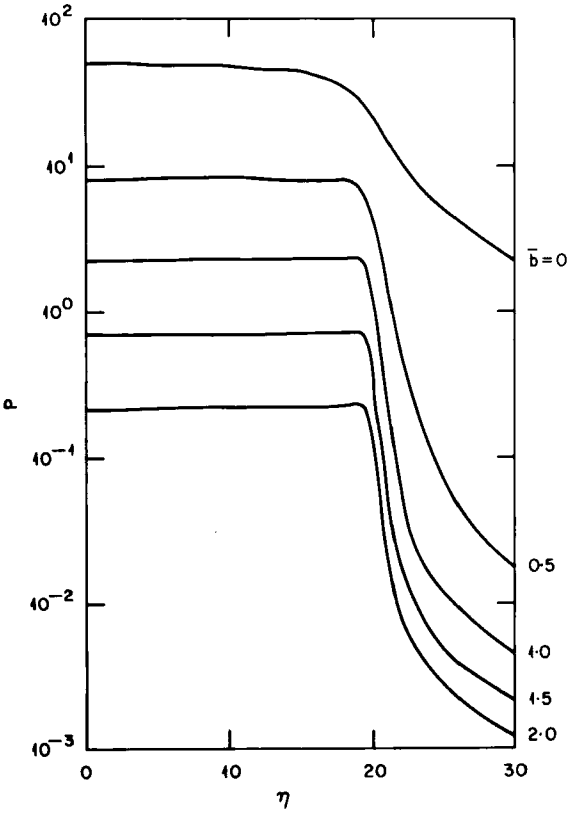

A plot of p, the differential probability of exciting a surface collective mode, as a function of the scaled collection angle $\eta=2E\theta_y/\hbar\omega_s$ for the step function profile in eqn. (31), $\gamma_0=20$ and $\xi=1$.

Fig. 6

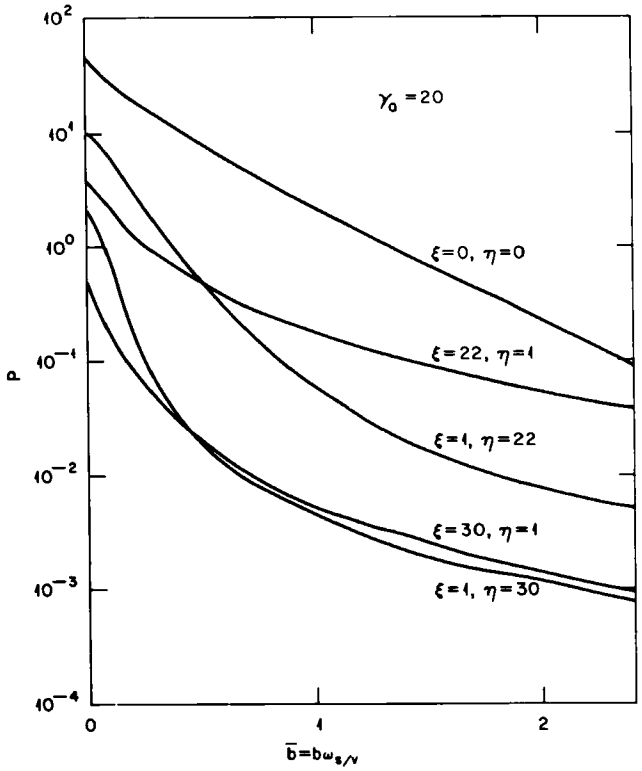

A plot of p against $\omega_s b/v$ for the step function profile in eqn. (31) for various angles of collection of the inelastically scattered electrons. The dimensionless impact parameter $\bar{b}=\omega_s b/v$, so that $\bar{b}\leqslant 1$ corresponds to $b=12{\cdot}3$ nm for 100 keV electrons exciting surface plasmons with an eigenenergy of 10 eV.

§6. Conclusions

For the simple axial detector configurations generally employed, the theory presented here establishes close and simple connections between the classical model of excitation and the more elaborate treatment based on a localized microprobe wave state. With off-axis positions, both models predict different degrees of improved spatial resolution of variations in excitation probability. In all detector positions the width Δ of the microprobe emerges from the wave theory as an obvious limit to the resolution attainable.

Spatial variations in elastic scattering and inelastic scattering frequently accompany one another and, although the former effect has for simplicity been ignored here, it may often be a factor which makes a full wave calculation necessary, particularly if crystalline diffraction effects occur. Finally the difficult problem of constructing a fully satisfactory model for the excitation of a medium whose properties vary continually in space has not been considered here and is a subject for future investigation.

Acknowledgments

This work was sponsored in part by the Office of Health and Environmental Research, U.S. Department of Energy, under Contract DE-AC05-840R21400 with

Martin Marietta Energy Systems, Inc., and in part by a Royal Society Guest Research Fellowship. R.H.R. thanks John C. Inkson, the Microstructure Physics Group, and the TCM group, Cavendish Laboratory, for their kind hospitality during the time that this work was done. Comments by L. D. Marks and V. W. Maslen are gratefully acknowledged. Partial support from NATO Research Grant No. 0142/87 is acknowledged.

References

Batson, P. E., 1980, *Solid St. Commun.*, **34,** 477; 1982a, *Phys. Rev. Lett.*, **49,** 936; 1982b, *Ultramicroscopy*, **9,** 277.

Brown, L. M., 1981, *J. Phys.* F, **11,** 1.

Colliex, C., 1985, *Ultramicroscopy*, **18,** 131.

Cowley, J. M., 1982, *Phys. Rev.* B, **25,** 1401.

Craven, A. J., Gibson, J. M., Howie, A., and Spalding, D. R., 1978, *Phil. Mag.* A, **5,** 519.

Das, P. C., and Gersten, J. I., 1983, *Phys. Rev.* B, **27,** 5412.

Echenique, P. M., 1985, *Phil. Mag.* B, **52,** L9.

Echenique, P. M., Bausells, J., and Rivacoba, A., 1987, *Phys. Rev.* B, **35,** 1521.

Echenique, P. M., and Howie, A., 1985, *Ultramicroscopy*, **16,** 269.

Echenique, P. M., and Pendry, J., 1975, *J. Phys.* C, **8,** 2936.

Egerton, R. F., 1980, *Ultramicroscopy*, **5,** 521.

Ferrell, T. L., and Echenique, P. M., 1985, *Phys. Rev. Lett.*, **55,** 1526.

Howie, A., Linington, P. F., and Tomlinson, P. N., 1971, *Phil. Mag.*, **23,** 1559.

Howie, A., and Milne, R. H., 1985, *Ultramicroscopy*, **18,** 427.

Isaacson, M., and Johnson, D., 1975, *Ultramicroscopy.*, **1,** 33.

Joy, D. C., 1979, *Introduction to Analytical Electron Microscopy*, edited by J. J. Hren, J. I. Goldstein and D. C. Joy (New York: Plenum), p. 223.

Kohl, H., 1983, *Ultramicroscopy*, **11,** 53; 1985, *J. Microsc. Spectroscopy Electron.*, **10,** 431.

Krivanek, O. L., Tanishiro, Y., Takayangagi, K., and Yagi, K., 1983, *Ultramicroscopy* to be published.

Mahan, G. D., 1974, *Elementary Excitations in Solids, Molecules and Atoms*, Vol. B, edited by J. T. Devreese, A. B. Kunz and T. C. Collins (New York: Plenum), p. 93.

Metherell, A. J. F., 1971, *Advances in Optical and Electron Microscopy*, Vol. IV, edited by V. E. Cosslett and R. M. Bauer (New York: Academic Press), p. 263.

Ritchie, R. H., 1981, *Phil. Mag.* A, **44,** 931.

Ritchie, R. H., and Marusak, A. L., 1966, *Surf. Sci.*, **4,** 234.

Ritchie, R. H., and Wilems, R. E., 1969, *Phys. Rev.*, **178,** 372.

Scherzer, O., 1949, *J. appl. Phys.*, **20,** 20.

Schmeits, M., 1981, *J. Phys.* C, **14,** 1203.

Taftø, J., Krivanek, O. L., Spence, J. C. H., and Honig, J. M., 1982, *Phys. Rev. Lett.*, **48,** 560.